FLOW PATTERNS WITHIN A SLOPING PERCHED WATER IN A GRADUALLY LAYERED SOIL

Stefano Barontini[1], Marco Peli[1] & Roberto Ranzi[1]

[1]DICATA, University of Brescia, Italy, Via Branze 43, I—25123
E-mail: barontin@ing.unibs.it

Abstract

The onset of a perched water table in a sloping soil, during rainfall events, is one of the most important landslides triggering mechanisms. As perched water tables are mostly induced by the decreasing of the hydraulic conductivity at soil saturation with depth, in this paper we will present some results on the effect of gradually decreasing conductivity on the flow due to a steady infiltration process in a sloping and a priori anisotropic soil, laying on a capillary barrier. On the basis of an application of the Darcy law, the flow field within the perched water is analytically solved and the corresponding Lagrange stream function is determined. The flow patterns are calculated and presented for the particular case of exponentially decreasing hydraulic conductivity at saturation with depth.

Introduction

The formation of perched water tables in the upper soil layers, during an infiltration process at low infiltration rate, is an important shallow—landslide triggering mechanism. In fact, when the soil approaches the saturation degree in the upper soil layers, the apparent cohesion reduces and, when it reaches the saturation, also the effective strengths reduce. Soil failures can therefore be triggered both by a positive pore pressure and by the presence of soil layers close to saturation (e.g. van Asch et al., 2009). Perched water tables are typically induced by the layering of the soil water constitutive laws and mostly by the decreasing of the hydraulic conductivity at soil saturation with depth. An accurate description of the subsurface soil—water flow, which accounts also for the effect of the unhomogeneities of the soil hydraulic properties, therefore leads to important information on the properties of the perched water tables and on the soil safety.

As a consequence of the genetic layering, the conductivity at saturation tends to decrease across the upper soil horizons, being higher in the A horizon and lower in the B one (Kirkby, 1969). On mountains, where strong erosive processes act and mass movement is a key soil forming factor, the soil horizonation cannot fully develop and a smooth decrease of the conductivity at saturation typically occurs in the upper soil layers. During our field measurement campaigns in two Alpine catchments, a gradual decrease, on average, was observed for the vertical conductivity at saturation through the upper soil layers (Barontini et al., 2005). Consistent with literature data (e.g. Beven, 1984), the pattern was found to be reasonably approximated by an exponential decay.

Below the upper soil layers, two limit cases can describe the soil characteristics: one can find either an impervious bedrock, or a highly permeable layer of regolith or fractured and fissured rock. In the first case, and in case of formation of a perched water table, the maximum pressure head is expected to be observed at the interface between the soil and the bedrock. If the slope is moderate, the flow description can be performed by means of a classical Dupuit—Forchheimer approach, leading in the saturated layer to a Boussinesq equation (e.g. Steenhuis et al., 1999). In the second case, instead, the soil behaves like a porous layer on a capillary barrier, and the maximum pressure head, if any exists, will be found within the soil. The transverse flow across the soil layer can be a priori not negligible and one of the major Dupuit—Forchheimer hypotheses may fail. An approach based on the Richards equation, and on its simplifications for the saturated flow, is therefore needed in these cases. According to Zaslavsky and Sinai (1981) the problem can be simplified, for a long slope, with a uniform flow, in which the flow field has both a lateral component, parallel to the slope, and a transverse one. Following this approach the infiltration thresholds for the perched water table to onset and to lead the soil to waterlogging were determined for a sloping, anisotropic and gradually non homogeneous soil, together with other characteristic properties of the perched water table (Barontini et al., 2011). Here, after a recall of the underlying hypotheses and of previous results, the Lagrange stream function of the flow field is presented and its patterns discussed in relation with their physical meaning.

Theoreticals

Problem statement

Let us consider a finite thickness soil layer laying on a hillslope, tilted of an angle β with the horizontal as represented in Fig. 1. Let x^* be the intrinsic transverse

coordinate, such that $x^* = 0$ at the soil surface and x^* is positive as entering within the soil. Say x_f^* the position of the soil bottom. Let the soil be seat of Darcian fluxes:

$$\mathbf{q} = -\mathbf{K}(\eta, x^*)\nabla\Phi\,, \tag{1}$$

where $\mathbf{q} = (q_{x^*}, q_{y^*})$ is the apparent flow field within the soil layer, $\mathbf{K}(\eta, x^*)$ is the soil hydraulic conductivity tensor, depending on the tensiometer—pressure potential η and on the depth x^*, and $\Phi = \eta - z$ is the total soil—water potential (z as represented in Fig.1). We recall that η is defined as the matric potential, if it is non—positive, or as the pressure potential, otherwise. With the hypotheses that the soil unhomogeneities are fully represented by a decreasing of the soil conductivity at saturation with depth, and that the soil intrinsic coordinates x^* and y^*, as represented in Fig. 1, are principal direction for the conductivity tensor, $\mathbf{K}(\eta, x^*)$ is therefore defined as:

$$\mathbf{K}(\eta, x^*) = k(\eta)\begin{bmatrix}1 & 0\\ 0 & r\end{bmatrix}K_S(x^*), \tag{2}$$

being $k(\eta)$ the relative conductivity, r the anisotropy factor and $K_S(x^*)$ the hydraulic conductivity at soil saturation in the transverse direction x^*. If the soil is saturated, i.e. $\eta > 0$, $k(\eta)$ is equal to 1. Due to the soil genetic processes, the ratio r between the lateral and transverse conductivity at saturation is usually higher than 1. Let $K_S(x^*)$ be monotonically decreasing and be described by the following equation:

$$K_S(x^*) = K_{S,o}f(x^*), \tag{3}$$

in which $K_{S,o}$ is the conductivity at saturation at the soil surface $x^* = 0$ and $f(x^*)$ is a monotonically decreasing function such that $f(0) = 1$.

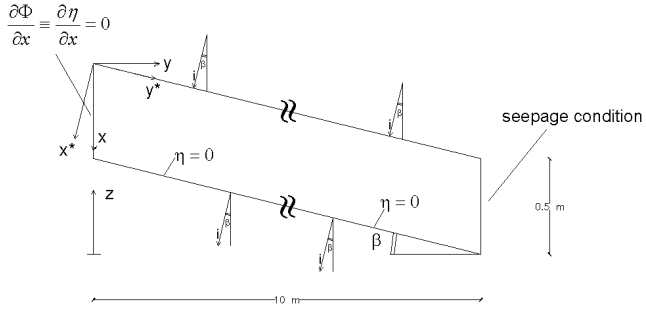

Figure 1: Sketch of a soil domain with details on the boundary conditions

Let the soil lay on a capillary barrier, i.e. let the underlying soil layer be characterized by higher conductivity than $K_S(x_f^*)$ and let it be not able to exercise any retention. For the sake of continuity of the total hydraulic head Φ, the tensiometer—pressure potential $\eta(x_f^*)$ should be null.
Now let i be the rainfall component normal to the soil surface. With the aforementioned condition for the lower boundary of the domain, i.e. $\eta(x_f^*) = 0$, a perched water is considered to onset if:

$$\left.\frac{\partial\eta}{\partial x^*}\right|_{x_f^*} < 0\,. \tag{4}$$

Consistent conditions at the lateral boundary of the domain are a no flux entering the domain at the upstream boundary, as for the presence of a watershed, and a seepage condition at the downstream boundary, as represented in Fig.1.
In one of their 1981's papers, Zaslavsky and Sinai (1981) described the effect of an infiltration process in a soil layer of undefinite length – laying on a sloping capillary barrier and eventually anisotropic and sharply layered – as a flow with uniform properties in the y^* direction, with deflected patterns from the transverse direction due to the soil slope, to the K_S profile and eventually to the soil anisotropy. The uniform flow condition takes the form:

$$\frac{\partial}{\partial y^*}(\cdot) = 0 \tag{5}$$

for all the flow properties unless than for the gravitational potential $-z$.

Flow fields

As steady conditions are investigated, the continuity equation takes the form:

$$\nabla\cdot\mathbf{q} = 0. \tag{6}$$

For the sake of continuity, accounting for the condition (5) applied to q_{y^*}, one gets from (6):

$$q_{x^*} = i\,, \tag{7}$$

for each x^*. Then, by the Darcy law (1) with the condition (5) applied to η, one gets:

$$q_{y^*} = K_{s,o}\, k(\eta)\, r\, f(x^*) \sin\beta\,. \tag{8}$$

It can be observed that the flow field is uncoupled in the two directions, i.e. the two flow components can be separately solved. In fact q_{y^*} depends on the boundary condition i only as a function of the tensiometer—pressure potential profile $\eta\,(x^*)$ which is a solution of the Darcy law with the condition (7).

Properties of a perched water table

Accounting for the hypothesis (5), Barontini et al. (2011) showed and numerically verified that the infiltration threshold $i_f\,(\beta)$ for the perched water to onset is given by:

$$i_f(\beta) = K_S\left(x_f^*\right)\cos\beta, \tag{9}$$

i.e. it is equal to the conductivity at the bottom of the soil layer, scaled with the cosine of the slope. This infiltration rate is less than the expected one in the case of horizontal soil, due to the fact that the gravitational gradient, sustaining the flux transversely to the soil layer, is less effective as the slope increases. The maximum infiltration, which can be sustained without gaining any negative pressure gradient at the lower soil interface, will be reduced accordingly. The infiltration rate leading to waterlogging is related to the value of the equivalent hydraulic conductivity at saturation over the interval [0, x_f*], i.e.:

$$i^*(\beta) = K_{S,eq}^{\left[o,x_f^*\right]}\cos\beta = K_{S,o}\frac{x_f^*}{\int_o^{x_f^*}\frac{dx'}{f(x')}}\cos\beta \tag{10}$$

and, again, it is scaled with the cosine of the slope. The authors proved also that the profile of $\eta(x^*)$ within the perched water is not monotonic and it has a maximum η_{max} in a position x^*_{max}. The position x^*_{max} is given by:

$$i = K_S(x^*_{max})\,,\, i_f(\beta) < i \le i^*(\beta), \tag{11}$$

thus not depending on the soil slope β. The corresponding η_{max} is found by a straight integration of the Darcy law within the saturated layer:

$$h_{max}(\beta) = \\ = \left[\int_{x^*_{max}}^{x_f^*}\frac{i}{K_S(x')}\,dx' - \left(x_f^* - x^*_{max}\right)\right]\cos\beta\,. \tag{12}$$

It is here remarked that all the properties given by equations (9—12) are not dependent on the soil anisotropy as a consequence of the flow components uncoupling. The soil anisotropy acts in fact on the lateral flow, while these properties pertains the transverse flow.

Lagrange stream function

As a consequence of the continuity equation (6) the flow field **q** admits a vector potential $\boldsymbol{\psi}(x^*, y^*)$ i.e. it can be written as:

$$\mathbf{q} = \nabla \times \boldsymbol{\psi}. \tag{13}$$

By defining z^* as the orthogonal coordinate to the plane identified by x^* and y^*, positive if coming out from the sheet, it can be proven that, in the case of a steady planar flow, the vector potential has only a component parallel to z^*. It can therefore be written as:

$$\boldsymbol{\psi} = \psi_{z^*}\mathbf{k}, \tag{14}$$

being **k** the unitary vector of the z^*-axis and $\psi_{z^*}\,(x^*, y^*)$ the Lagrange stream function. It can be also proven that ψ_{z^*} can be determined as a line integral of the flow field **q** along a path l:

$$\psi_{z^*}(x^*, y^*) = \int_{\mathbf{x_o}}^{\mathbf{x}} \mathbf{q}\cdot\mathbf{n}\,dl + \psi_{z^*}(x_o^*, y_o^*), \tag{15}$$

where $\boldsymbol{x} = (x^*, y^*)$ and $\boldsymbol{x_o} = (x_o^*, y_o^*)$ are the coordinates of two points and **n** is the unitary vector orthogonal to the integration path.

Let us assume now $\boldsymbol{x}_o = \boldsymbol{x}_f = (x_f^*, 0)$. As the components of **q** are expressed by equations (7, 8), the general form for the Lagrange stream function is given by the following equation:

$$\psi_{z^*}(x^*, y^*) = \\ = K_{S,o} r \sin\beta \int_{x_f^*}^{x^*} k(\psi) f(x^{*\prime})\,dx^{*\prime} - i y^* \\ + \psi_{z^*}\left(x_f^*, 0\right). \tag{16}$$

As the iso—lines of ψ_{z^*} are locally parallel to the flow field **q** by definition, the first term of equation (16) accounts for the flow path divergence from the vertical direction due to the slope and to the soil anisotropy.

Case of exponentially decreasing conductivity

Equations (9—12) and (16) are of general validity and only require the shape of $f(x^*)$ to be given, in order to determine the properties of the perched water table. If the soil conductivity at saturation exponentially decreases with depth with a constant of exponential decay L, equation (3) takes the form:

$$K_S(x^*) = K_{S,o} e^{-\frac{x^*}{L}} \tag{17}$$

Equation (17) allows to determine the numerical values given by equations (9—12), as in Barontini et al. (2011).

If we consider a waterlogging condition, in all the domain the soil is saturated and it is $k(\eta) = 1$. Equation (16) can therefore be explicitly solved, thus obtaining:

$$\psi_{z^*}(x^*, y^*) = -K_{S,o} r L \sin\beta \left(e^{-\frac{x^*}{L}} - e^{-\frac{x_f^*}{L}} \right) - i y^* + \psi_{z^*}\left(x_f^*, 0\right) \tag{18}$$

Assuming:

$$\psi_{z^*}\left(x_f^*, 0\right) = -K_{S,o} r L \sin\beta \, e^{-\frac{x_f^*}{L}} \tag{19}$$

one finally gets the Lagrange stream function for the investigated problem:

$$\psi_{z^*}(x^*, y^*) = -K_{S,o} L r \sin\beta \, e^{-\frac{x^*}{L}} - i y^*. \tag{20}$$

As the drop will follow an iso—line of ψ_{z^*}, the distance along the slope between the point at which a drop enters the saturated layer and the point at which it leaks out can be directly determined from (20).

Results

Some typical flow patterns within a perched water table at waterlogging, derived by means of equation (20), are presented in Fig. 2 for different values L, r and β. In order to plot the iso—lines of ψ_{z^*}, the following dimensionless variables were defined:

$$X^* = \frac{x^*}{x_f^*}, Y^* = \frac{y^*}{x_f^*}, \quad \Pi_L = \frac{L}{x_f^*}, \Pi_i = \frac{i}{K_{S,o}}, \quad \Psi_{z^*} = \frac{\psi_{z^*}}{x_f^*}. \tag{21}$$

By means of the definitions (21), the infiltration rate at waterlogging $i^*(\beta)$, given by equation (10) with the constitutive law (17), can be rewritten in the following form, according to Barontini et al. (2012):

$$\Pi_{i^*}(\beta) = \frac{1}{\Pi_L \left(e^{\frac{1}{\Pi_L}} - 1 \right)} \cos\beta \, . \tag{22}$$

Equation (20) is therefore rewritten as:

$$\Psi_{z^*}(X^*, Y^*) = -\Pi_L r \, \sin\beta \, e^{-\frac{X^*}{\Pi_L}} - \Pi_i Y^*. \tag{23}$$

The flow patterns were presented both for weakly unhomogeneous soils (Π_L = 0.5, upper four diagrams) and for strongly unhomogeneous ones (Π_L = 0.2, lower four diagrams), in case of moderate (β = 5°, first and third lines) and steep slope (β =30°, second and forth lines), and for isotropic soils (left side diagrams) and strongly anisotropic ones (r = 10, right side diagrams).

In the case of isotropic and moderately sloping soils (β = 5°) the water infiltrating at the upper surface of the perched water table rapidly leaks toward the underlying soil. Accounting for the tilting of the slope the paths are almost vertical for moderately unhomogeneous soil (Π_L = 0.5). As soon as the soil is more unhomogeneous (Π_L = 0.2) the paths diverge downstream of a stretch of the same order of magnitude of the soil thickness. As the slope becomes steeper (30°) this pattern is emphasized and, for strongly decreasing conductivity with depth (Π_L = 0.2), the lateral bias is between three and four times the soil thickness.

The same behavior characterizes anisotropic soils in moderately steep slopes. In fact the paths diverges downstream as the anisotropy factor increases. For strong anisotropy (r = 10) and moderately steep slope (5°) the lateral bias ranges from one to five times the soil thickness, for weakly and strongly unhomogeneous soil respectively. Finally if the soils are both steep sloping and anisotropic the effects superimpose and the paths strongly diverges downstream. The lateral bias is about eight times the thickness if Π_L = 0.5 and becomes about thirty times if Π_L = 0.2 but it remains in any case finite.

Natural slopes are often thin if compared with their length. This is why in the diagrams in order to represent a central branch of natural slopes, the slope length is twenty times the thickness. As in most of the cases the water is able to reach the bottom layer with a lateral bias of few thicknesses, it can be hypothesized that the uniform flow approach is a physically meaningful framework for real cases of flow across a perched water laying on a capillary barrier. On the contrary, as the transverse flow is valuable in the whole domain in most of the cases, it is confirmed that a classical Dupuit—Forchheimer approach cannot apply.

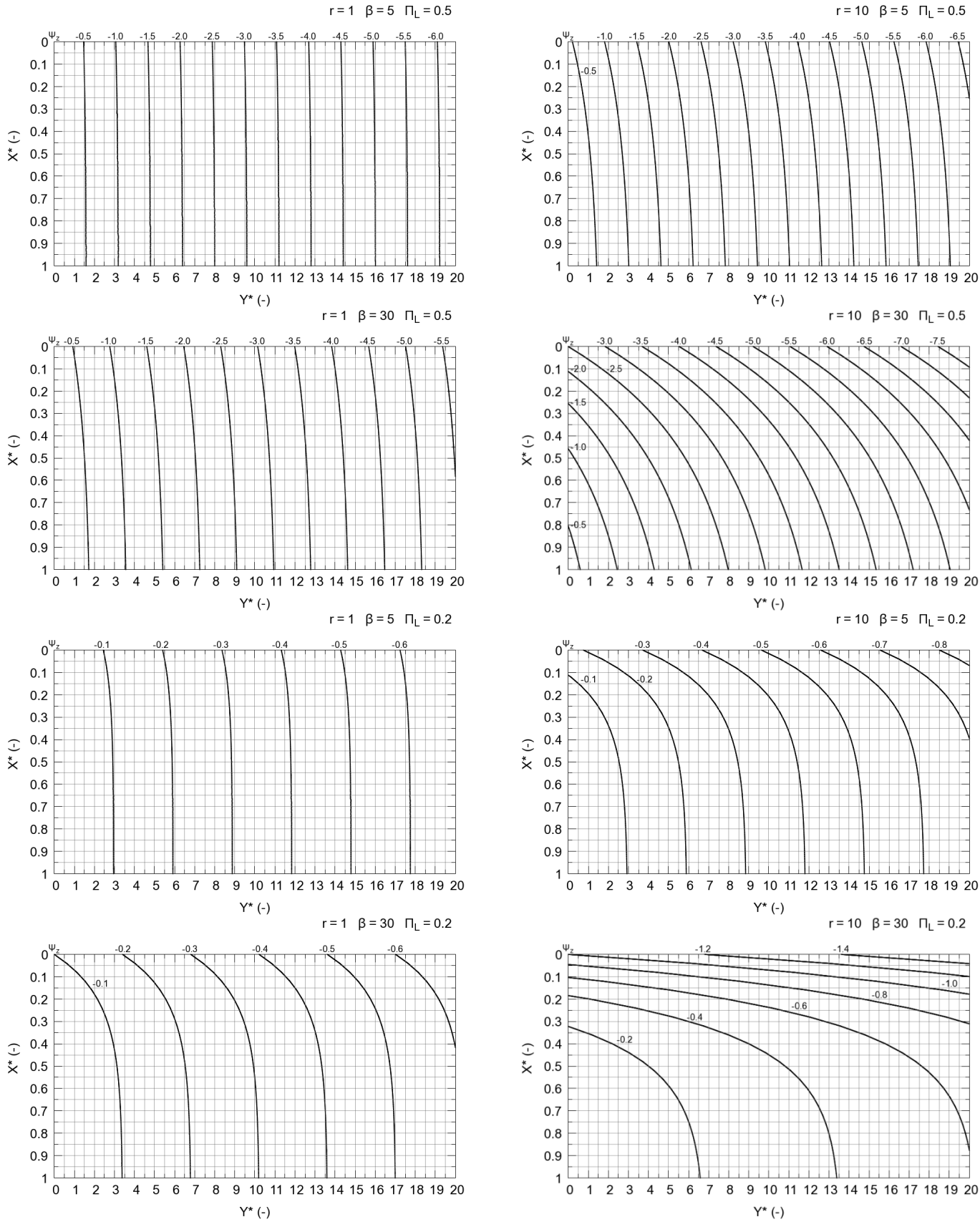

Figure 2: Iso—lines of the normalized Lagrange stream function Ψ_{z^*} as described by equation (23) for different soils (r = 1, 10; β = 5°, 30°; Π_L = 0.2, 0.5)

Conclusions

Aiming at better characterizing the physical aspects of the flow within a perched water table, in view of application to soil stability analyses, the case of a gradually unhomogeneus and a priori anisotropic sloping soil, laying on a capillary barrier, was theoretically investigated. The soil unhomogeneity was assumed to be described by the decreasing of the hydraulic conductivity at saturation with depth. By means of a uniform flux approach, the flow field and the stream function within the perched water table were theoretically determined for any soil with monotonically decreasing conductivity with depth.

The particular case of a soil at waterlogging with exponentially decreasing conductivity with depth was afterwards investigated and the flow patterns presented. It was observed that for weakly unhomogeneous and isotropic soil laying on a moderately steep slope, the water infiltrated at the soil surface rapidly reaches the soil bottom along almost vertical paths. As the slope steepness, the unhomogeneity and the anisotropy increase, the paths diverge downstream with a bias ranging from few times to some tenths the soil thickness.

The paths remain in any case finite and a drop of water infiltrated at the soil surface is able to leak out downstream. The estimates of the lateral bias suggested that the uniform flow approach can be a physically meaningful framework to describe the water content flow in natural soils laying on a sloping capillary barrier, but the importance of the transverse flow component confirmed that a classical Dupuit—Forchheimer approach does not apply in this case.

Acknowledgements

This research was founded by the FP7 Project KULTURisk under the grant agreement EC 265280. One of the authors was partially founded also by the Italian Ministry of Foreign Affairs within the research grant CUP D81J11000160006.

References

Barontini S., Clerici A., Ranzi R., Bacchi B. (2005) Saturated hydraulic conductivity and water retention relationships for Alpine mountain soils. *Climate and Hydrology of Mountain Areas*. De Jong C, Collins D, Ranzi R (eds). J. Wiley and Sons, Ltd., Chichester, West Sussex, England. (ISBN_0-470-85814-1_) pp. 101—122.

Barontini S., Peli M., Bakker M., Bogaard T. A., Ranzi R. (2011) Perched waters in 1D and sloping 2D gradually layered soils. First numerical results. Proceedings of the XXth Congress of AIMETA, Bologna, Italy.

Barontini S., Peli M., Bogaard T. A., Ranzi R. (2012) Dimensionless numerical approach to perched waters in 2D gradually layered soils. *Proceedings of the Second World Landslide Forum – 3-7 October 2011, Rome*, in press.

Beven K. J. (1984) Infiltration into a class of vertically non-uniform soils. *Hydrological Science Journal — Journal des Science Hydrologique Bulletin* 24, pp. 43—69.

Kirkby M (1969) Infiltration, throughflow and overland flow. *Water, Earth and Man*. Chorley R (eds). Taylor & Francis. pp. 215—227.

Steenhuis T. S., Parlange J.-Y., Sanford W. E., Heilig A., Stagnitti F., Walter M. F. (1999) Can we distinguish Richards' and Boussinesq's equations for hillslopes?: The Coweeta experiment revisited. *Water Resources Research*. 35.2, pp. 589—593.

Van Asch Th. W. J., L. P. H. Van Beek, T. A. Bogaard (2009) The diversity in hydrological triggering systems of landslides. Rainfall-induced landslides. Mechanisms monitoring techniques and nowcasting models for early warning systems. *Proceedings of the 1st Italian Workshop on Landslides*. Picarelli L, Tommasi P, Urciuoli G, Versace P (eds). Vol.1. Napoli.

Zaslavsky D., Sinai G. (1981) Surface Hydrology: III—Causes of Lateral Flow. Journal of the Hydraulic Division, ASCE, Vol. 107, No. HY1, Proc. Paper 15960, Jan., 1981, pp. 37—52.